J Mater Sci (2011) 46:2479–2487
DOI 10.1007/s10853-010-5096-x

Effect of interface bonding on the phase-transformation-aided magnetoelectric effect in ferromagnetic/ferroelectric composites

Rui-Hong Wang · Guo-Jun Zhang · Mai-Qun Zhao

Received: 2 May 2010 / Accepted: 18 November 2010 / Published online: 4 December 2010

Abstract Based on modified constitutive equations and finite element method, calculations have been performed to study the effect of interface bonding on the phase-transition-aided magnetoelectric (ME) response in a new kind of NiMnGa/lead–zirconate–titanate (PZT) multiferroic laminate composites. The results quantitatively show that the ME effect is remarkably dependent on both the interface layer characteristics and the interface layer thickness. Stiffer and thinner interface layers are apt to produce higher ME effect. Calculations are in good agreement with available experimental results. Furthermore, the theoretical approach was improved to consider the enhancement in the magnetostriction of martensites induced by pre-applied opposing stress. Predictions reveal that the usage of single crystal Fe_7Pd_3 as ferromagnetic phase to form magneto-electric composite with PZT can produce a high ME up to ~ 1 V/cm Oe.

Introduction

Multiferroic materials [1–3] have drawn increasing interest due to their multi-functionality, which provides significant potentials for using as next-generation multi-functional devices. The characteristic of these multiferroic materials is the coupling interaction between the multiferroic orders to produce some new effects, such as magnetoelectric (ME) effect [4, 5]. The ME response is an appearance of an electric polarization upon applying a magnetic field and hence the electric polarization of ME materials will be variant with external magnetic field [6, 7]. The ME effect was prophetically predicted by Pierre Curie early in 1894 on the basis of crystal symmetry consideration [8]. However, no further work was done until 1958 when Landau and Lifshitz proved the feasibility of the ME effect in certain crystals. Subsequently, the symmetry argument was applied by Dzyaloshinskii [9] to antiferromagnetic Cr_2O_3 and it was suggested that the ME effect could appear in Cr_2O_3, which was followed by experimental confirmation [10]. Since then, the ME effect has been investigated in some monophase materials with different crystal families, including antiferromagnetic Cr_2O_3, yttrium iron garnets, boracites, rare-earth ferrites, and phosphates [11]. Most recently, theoretical breakthrough [12, 13] in understanding the coexistence of magnetic and electrical ordering in single-phase multiferroics have shown that the usual atomic-level mechanisms driving ferromagnetism and ferroelectricity are mutually exclusive, because they require empty and partially filled transition metal orbitals, respectively. This recognition has promoted the search for alternative ferroelectric mechanisms that are compatible with the occurrence of magnetic ordering [5]. As a result, some new single-phase multiferroics have been discovered. For example, the form of ferroelectric phase transitions induced by magnetic fields have been observed in perovskite manganites [2] while ferromagnetism induced by electric fields in hexagonal manganites [14]. However, these monophase ME materials are not very attractive for application in short term, because they do not exhibit strong ME effect (e.g., the largest ME coefficients that have been observed in monophase ME materials is only about 6×10^{-3} V/cm Oe in $PbPO_4$ [7, 15]) and most of them have rather low Neel or Curie temperature far below room temperature.

R.-H. Wang (✉) · G.-J. Zhang · M.-Q. Zhao
School of Material Science & Engineering, Xi'an University of Technology, Xi'an 710048, China
e-mail: wangrh@mail.xjtu.edu.cn

Alternatively, some multiferroic composites made by combining ferromagnetic (magnetostrictive) and ferroelectric (piezoelectric) substances together, such as ferrite/titanate [16, 17] and ferrite/lead–zirconate–titanate (PZT) [18, 19], have been recently found to exhibit an extrinsic ME effect, resulting from a coupling interaction between the ferromagnetic and ferroelectric substances. These multiferroic composites could have ME effect much larger (orders of magnitude higher) than the monophase ME materials and could be used in room temperature, which makes them have more possible applications such as in sensor, actuators, and transducers [20–22]. Special attention has been paid on the laminated magnetostrictive/piezoelectric multiferroic composites mainly because of their much simple but favorably repeatable preparing procedure [7]. The piezoelectric phase and magnetostrictive phase could be prepared, respectively, and be bonded by using interfacial binder such as silver epoxy [23] and conductive epoxy [24]. The magnetic-field-induced strain in the magnetostrictive phase could be transferred through the interfacial binder layer to the piezoelectric phase, resulting in an induced voltage. In other words, the ME effect in the laminated magnetostrictive/piezoelectric multiferroic composites is a product tensor property, not intrinsic to individual phases, combining the magnetoelastic effect and elastoelectric effect of individual phases, via an elastic coupling within the interfacial binder layer.

The ME effect of the laminated magnetostrictive/piezoelectric multiferroic composites is strongly dependent on the characteristics and volume fraction (thickness fraction) of the two constituent phases. It can yield a large ME response with use of magnetostrictive phase with giant magnetic-field-induced strain as well as of the piezoelectric phase with high elastoelectric response. Thicker magnetostricitve phase layer will also increase the ME effect because it is more ease for the magnetostrictive strain to drive the thinner piezoelectric phase layer to deform elastically. As a leading magnetostrictive material, rare-earth-iron alloy $Tb_{1-x}Dy_xFe_2$ (Terfenol-D) has been availably used as the magnetostricitve phase in the laminated multiferroic composites due to its giant magnetostrictive strain up to about 1000 ppm at a magnetic field of over 1200 Oe [25]. Ryu et al. [23, 26] have prepared the laminated Terfenol-D/PZT multiferroic composites and obtained a large ME coefficient of about 4.68 V/cm Oe at $t_m/t = 0.8$, where t_m is the thickness of the magnetostrictive layer and t the total thickness of the laminated composite. Mori and Wuttig [24] chose the Terfenol-D and polyvinylidenefluoride (PVDF) as the magnetostrictive and piezoelectric layers for laminated multiferroic composites, respectively, and observed a ME coefficient of 1.43 V/cm Oe at $t_m/t = 0.96$. Dong et al. [26] used a $\langle 001 \rangle$-oriented $0.7Pb(Mg_{1/3}Nb_{2/3})O_3$–$0.3PbTiO_3$ (PMN–PT) piezoelectric single crystal as the ferroelectric phase and measured a ME coefficient of 2.2 V/cm Oe in the laminated Terfenol-D/PMN–PT multiferroic composites at $t_m/t = 0.5$. Other magnetostrictive materials, such as Permendur [27], Fe–Ga [28], and $NiFe_2O_4$ [29], have been also bonded with PZT to produce a large ME coefficient of a similar magnitude. Most recently, high-permeability magnetostrictive FeBCSi alloy (relative permeability $\mu_r > 40000$) and FeSiCo alloy ($\mu_r > 120000$), instead of previous low-permeability magnetostrictive alloys (e.g., Terfenol-D having μ_r about only 3–10), have been used [27, 28] as magnetostrictive phase in the laminated multiferroic composites, which increase the ME coefficient even by a order of magnitude. The main reason for this remarkable increase is that the maximum effective piezomagnetic coefficient could be achieved under relative low magnetic biases in the high-permeability magnetostrictive materials. However, these iron-based alloys have the disadvantages of little field-induced strain (only about 27–45 ppm) and oxidation, which will limit their extensive applications.

Heusler alloy NiMnGa, exhibiting both the ferromagnetism and ferroelasticity properties, is another kind of favorable materials that could be served as the magnetostrictive phase in laminated multiferroic composites. With variation in temperature, the NiMnGa alloys will undergo a phase transformation from parent cubic structure to tetragonal structure of martensite and induce a large strain in the transformation course. This transformation-induced strain could be strongly enhanced by the application of magnetic field. The coupling of ferroelasticity and ferromagnetism in the NiMnGa alloys yields a giant so-called magnetic-field-induced strain. It has been reported that a large strain caused by the phase transformation at about 292 K could be up to 1.2×10^4 ppm in Ni_2MnGa single crystal samples without an applied magnetic field, and to 3×10^4 ppm by applying 0.6 T magnetic field [29]. The giant magnetic-field-induced strain observed in NiMnGa alloys is much larger than that could be achieved in Terfeniol-D ($\sim 1 \times 10^3$ ppm). It is thus expected that the use of NiMnGa alloys as magnetostrictive phase could remarkably enhance the output of electrical polarization in the laminated multiferroic composites (such as NiMnGa/PZT composites) and result in a giant ME effect.

However, a noticeable interface effect should be existed in the laminated ferromagnetic/ferroelectric composites and how the ME coefficient can achieve in the NiMnGa/PZT multiferroic composites is strongly dependent on the interface bonding. In this paper, by using modified constitutive equations, we employ a finite element method (FEM) to calculate the ME effect in the laminated NiMnGa/PZT composites, with aim to present the quantitative dependence of the ME response on interface bonding. Our simulation results show that a stiffer and thin interface layer is necessary to produce superior ME effect, which could be used to assist the design of multiferroic composites. This calculation method is also applicable to other laminated magnetostricitive/piezoelectric systems.

Theoretical framework

Consider the laminated NiMnGa/PZT composites, as shown in Fig. 1a. For the magnetostrictive phase, the magnetomechanical interaction is generally represented as

$$\begin{aligned}\sigma_{kl} &= c^{H}_{klij}\varepsilon_{ij} - \chi_{klmn}H_mH_n,\\ B_n &= \mu^{\varepsilon}_{nm}H_m + \chi_{ijmn}H_m\varepsilon_{ij},\end{aligned} \tag{1}$$

where σ is the stress, ε the strain, B the magnetic induction and H the magnetic field; c, μ, and χ are the stiffness at constant field, permeability tensor at constant strain, and magnetostrictive coefficient, respectively. For the magnetic-field-aided martensite transformation behavior in the NiMnGa phase, these coefficient tensors are somewhat dependent on the magnetic field, stress field, and temperature T [30]. Equation 1 can simply be rewritten as

$$\begin{aligned}\sigma_{kl} &= c^{H,T}_{klij}(\varepsilon_{ij} - \varepsilon^{M}_{ij}),\\ B_n &= \mu^{\varepsilon,T}_{nm}(\varepsilon, H, T)H_m,\end{aligned} \tag{2}$$

where the permeability μ depends on ε, H and T, and ε^M is the magnetic-field-aided martensite transformation strain of NiMnGa that is nonlinearly dependent on the temperature.

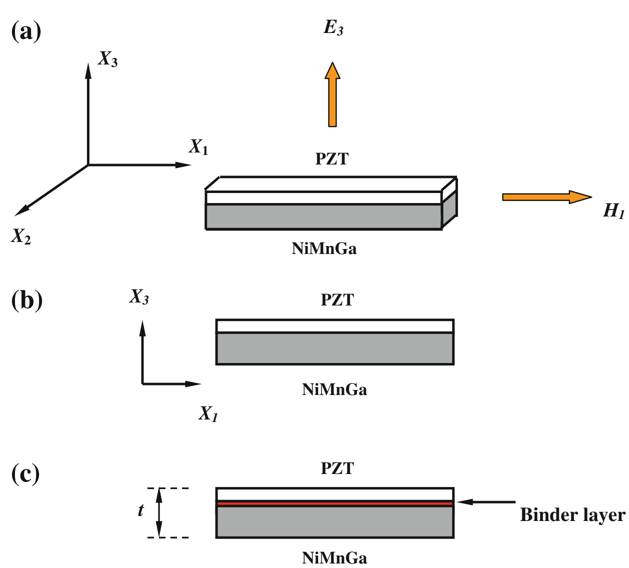

Fig. 1 **a** Triplanar sketch and definition of the coordination axes for the block-shaped laminate composite of NiMnGa and PZT. Cross section schematic illustration for bilayer NiMnGa/PZT composites without interface binder layer (**b**) and with interface binder layer (**c**)

On the other hand, for the piezoelectric phase layer, the electromechanical interaction is represented as

$$\begin{aligned}\sigma_{kl} &= c^{E}_{klij}\varepsilon_{ij} - \boldsymbol{e}_{ikl}\boldsymbol{E}_i,\\ \boldsymbol{D}_k &= \boldsymbol{e}_{kij}\varepsilon_{ij} + \boldsymbol{\kappa}^{\varepsilon}_{ki}\boldsymbol{E}_i,\end{aligned} \tag{3}$$

where $\boldsymbol{D}$ and $\boldsymbol{E}$ are the electric displacement and field tensor, respectively; $\boldsymbol{e}$ is the piezoelectric coefficient tensor; $\boldsymbol{\kappa}$ is the dielectric constant tensor at constant strain.

The response of laminated NiMnGa/PZT composite involving the magneto-electro-elastic coupling effect can be then described by the combination of Eqs. 2 and 3 with the following general equations, which is a modified version of former constitutive equations [31–33]

$$\begin{aligned}\sigma_{kl} &= c^{H,E,T}_{klij}\varepsilon_{ij} - \boldsymbol{e}^{H,T}_{ikl}\boldsymbol{E}_i - c^{H,E,T}_{klij}\varepsilon^{M}_{ij}\\ \boldsymbol{D}_k &= \boldsymbol{e}^{H,T}_{kij}\varepsilon_{ij} + \boldsymbol{\kappa}^{\boldsymbol{H},\varepsilon,\boldsymbol{T}}_{\boldsymbol{ki}}\boldsymbol{E_i} + \boldsymbol{\alpha}^{\boldsymbol{T}}_{\boldsymbol{ki}}\boldsymbol{H_i},\\ B_j &= \mu_{ji}(\varepsilon, \boldsymbol{E}, H, T)H_i,\end{aligned} \tag{4}$$

where the permeability, μ, depends on ε, magnetic and electric fields, and temperature; α is the ME coefficient and the superscript T indicates a temperature dependence associated with the phase transformation in NiMnGa. The strain ε, electric field, and magnetic field are, respectively, defined by the displacement u, electric potential φ, and magnetic potential ϑ, i.e.,

$$\varepsilon_{ij} = \frac{1}{2}(u_{i,j} + u_{j,i}), \quad \boldsymbol{E}_i = -\varphi_{,i}, \quad H_i = -\vartheta_{,i}, \tag{5}$$

The above constitutive equation, Eq. 4, is somewhat different from previous ones [31–33] because temperature-dependent and magnetic-filed-dependent phase transformation strain is considered in Eq. 4. While in previous constitutive equations, only the magnetostriction is only related to applied magnetic filed.

The magnetic flux density in the composites is dominantly induced by the externally applied magnetic field. In present FEM calculations, for simplification, μ_{ji} in Eq. 4 is considered as being only dependent on H. Thus, the finite element formulation can be described as

$$\left.\begin{bmatrix}[K_{uu}] & [K_{u\varphi}]\\ [K_{\varphi u}] & [K_{\varphi\varphi}]\end{bmatrix}\begin{Bmatrix}u\\ \varphi\end{Bmatrix}\right|_T = \left.\begin{Bmatrix}\boldsymbol{f} - [K_{uu}]\{\varepsilon^M\}\\ \boldsymbol{Q} - [K_{\varphi\vartheta}]\{\vartheta\}\end{Bmatrix}\right|_T \tag{6}$$

where the submatrices K_{uu}, $K_{u\varphi}$, $K_{\varphi\varphi}$, and $K_{\varphi\vartheta}$ indicate the elastic, piezoelectric, permittivity, and magnetoelectric coefficient matrices, respectively. $\boldsymbol{f}$ and $\boldsymbol{Q}$ represent mechanical excitation vector and electric charge vector related to mechanical loads and electric displacement, respectively, i.e., $\boldsymbol{f} = \int_V N^T_u P_v \mathrm{d}V + \iint_S N^T_u P_s \mathrm{d}S$ and $\boldsymbol{Q} = -\iint_S N^T_\varphi \boldsymbol{D}\mathrm{d}S$, where P_v and P_s are body force and surface force, respectively, N_u and N_φ are corresponding nodal shape functions. The superscript of T means a transpose in matrix. The left-hand side of Eq. 6 contains the unknown displacement and electric potential, and the right-hand contains the excitation of the structure in terms of mechanical load, applied magnetic load, and electric charge. Here, boundary conditions of open circuit (i.e., $D_3 = 0$) and end clamped in the electrical polarization direction (the 3-direction in Fig. 1a) are considered for complying with common experimental conditions. A commercial Ansys software package was employed to execute the calculations.

Results and discussion

Most recently, Zhao et al. [34] prepared bilayer composite of $Ni_2MnGa/PbZr_{0.52}Ti_{0.48}O_3$ using acrylic-modified epoxy as bonding layer and found an enhancement in the ME effect assisted by the martensite transition in Ni_2MnGa. The Ni_2MnGa alloy they used exhibits much less strain, as shown in Fig. 2a, compared with other giant magnetostrictive NiMnGa alloys mentioned above. This means that no failure at interface should be considered in their samples because of the low strain. In this section, we will first calculate the ME effect in the bilayer Ni_2MnGa/PZT composite, focusing on the influence of characteristics of the binder layer on the ME effect and without consideration of the interface failure. The calculation results will be compared with experimental measurements. Second, choosing much giant magnetostrictive NiMnGa alloys for calculations, we will focus on the dependence of GME effect on the interface failure or interface strength, from which it could be revealed that how the GME effect could achieve in the laminated magnetostrictive/piezoelectric multiferroic composites.

Influence of thickness and characteristics of binder layer

Coinciding with experiments [34], the geometrical configuration of block-shaped bilayer Ni_2MnGa/PZT composite in the present calculations is schematically shown in Fig. 1a, where an external magnetic field, H_1, is applied alone along the X_1-axis of the composite specimen and a ME output voltage E_3 is produced across the specimen along the X_3 direction. Thus, the ME sensitivity along the X_3 direction, α_{E31}^T, is

$$\alpha_{E31}^T = -\boldsymbol{E}_3/H_1|_T = \alpha_{31}^*/\boldsymbol{\kappa}_{33}^*|_T \tag{7}$$

where α_{31}^* and $\boldsymbol{\kappa}_{33}^*$ are the effective ME coefficient and dielectric constant of the composites, respectively. The magnetic-field-aided martensite transformation strain of a Ni_2MnGa block, ε^M, should be practically determined for a special sample and may be variable from each other. Here we employ the $\varepsilon^M - H - T$ behaviors measured by Zhao

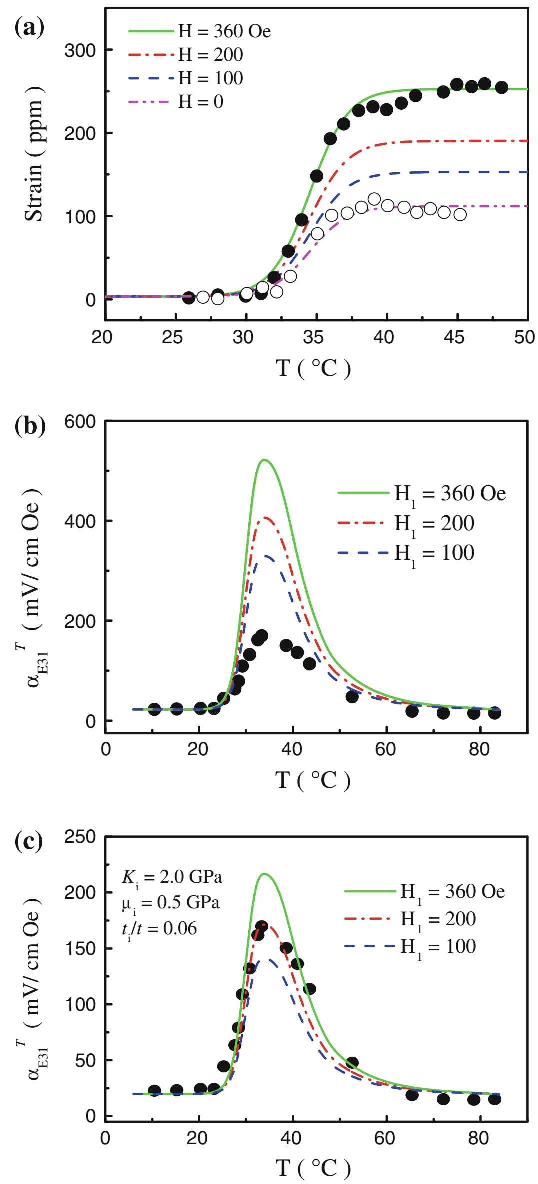

Fig. 2 **a** Dependence of the magnetic-field-aided martensite transformation of Ni_2MnGa alloy on the temperature as a function of the magnetic field. *Dots* are experimental results [34] and *curves* are fitting ones. **b** and **c** are the bias-dependent ME coefficient (α_{E31}^T) of the bilayer Ni_2MnGa/PZT composites without and with considering the influence of interface binder layer, respectively, corresponding to Fig. 1b, c. *Dots* are experiment results [34] and curves are from present calculations

et al. [34], as shown in Fig. 2a. One can notice that, without magnetic field, the saturation phase transformation strain during heating is about 100 ppm above the phase transformation temperature of about 37 °C. When applying a magnetic field of 360 Oe, the saturation phase transformation strain will increase to 250 ppm. Fitting lines are also given in the Fig. 2a to describe the dependence of ε^M on temperature as a function of magnetic field. For quantitative purposes, the other properties of the Ni_2MnGa and

Table 1 Properties of NiMnGa alloys and PZT used in the present FEM simulation [31, 34–36]

Properties	NiMnGa alloys	PZT
c_{11} (GPa)	157	121
c_{12} (GPa)	120	75.4
c_{13} (GPa)	120	75.2
c_{33} (GPa)	128	111
c_{44} (GPa)	107	21.1
$\varepsilon_{11}/\varepsilon_0$	–	916
$\varepsilon_{33}/\varepsilon_0$	–	830
e_{31} (C/m^2)	–	−5.4
e_{33} (C/m^2)	–	15.8
e_{15} (C/m^2)	–	12.3
μ_{33}/μ_0	5	–

the PZT used for calculations are presented in Table 1. Although the elastic modulus of the ferromagnetic Ni_2MnGa materials is somewhat dependent on the applied magnetic field [35] and temperature (phase transformation) [36], it is regarded as constant here for simplicity because the dependences are insignificant and the temperature range is somewhat narrow. Similarly, it is reasonable to assume that the elastic modulus of the epoxy layer is constant because it has been confirmed in an internal friction experiment [34]. The relative permeability and dielectric constant of the interfacial binder layers are both chosen as 6. Our FEM simulations showed that the calculated ME coefficients are quite insensitive to the permeability and dielectric constant of the interfacial layers, mainly due to two issues. One is that the ME response of the composites is due to the *mechanical* coupling between Ni_2MnGa and PZT and thus is dominated by the interfacial adhesion status. The other one is quite small thickness of the interfacial layers. The interfacial binder layers are just used to bond PZT and Ni_2MnGa for transferring the strain induced in Ni_2MnGa to PZT, and the elastic properties of the interfacial layers are far more vital than the relative permeability and dielectric constant in affecting the ME response. Thus, both the relative permeability and the dielectric constant of interfacial layers are chosen as 6 here for simplicity but without loss of generality.

For comparison reason, the assumption of perfect bonding is first considered, as shown in Fig. 1b. The perfect bonding means that the strain induced in NiMnGa phase could be completely transferred to the piezoelectric PZT phase and the elastic interaction between the two phases is ideal. In calculations, both the two blocks have the same width of 3 mm and length of 20 mm, but the NiMnGa block and PZT block have the thickness of 2 mm and 0.5 mm, respectively. All the model sizes are in accordance with experiments [34]. Figure 2b shows the calculated ME coefficient as a function of magnetic field. It is found that a higher magnetic field (e.g., 360 Oe) should yield a larger ME coefficient, which is attributed to the lager strain induced by the higher magnetic field (Fig. 2a). Depending on the temperature, the ME coefficient exhibits a vaulted shape with peak at about 40 °C, i.e., the phase transformation temperature. All the three α_{E31}^T versus T curves under different magnetic fields (100, 200, and 360 Oe) have a similar vaulted shape and all have a peak value at the same temperature. This indicates that, in the laminated Ni_2MnGa/PZT composite, the ME coefficient is dominated not only by the magnetic filed but also by the phase transformation in the Ni_2MnGa alloy, which is different from all the previous ferromagnetic/ferroelectric laminate composites that is merely dominated by the magnetic-field-induced strain in the ferromagnetic phase without the promotion of phase transformation [31–33].

Also presented in Fig. 2b (as dots) are the measurements of ME coefficient of the bilayer Ni_2MnGa/PZT composite under 216 Oe [34]. It is clearly found that the calculations (even under a magnetic field of 100 Oe) are much higher than the experimental results. This large discrepancy is mostly attributed to the neglecting of interface effect. Now turn to the second consideration of interface effect. Figure 1c schematically shows the layered multiferroic composite with interfacial binder layer, where t_i is the thickness of binder layer and t is the total thickness of the laminated composite. Some other important parameters of the binder layer are effective bulk and shear moduli, K_i and μ_i. The latter is especially important because it represents the capability to transfer the strain/stress from Ni_2MnGa to PZT. Different values will be used for μ_i in following calculations to reveal the influence of shear modulus on ME effect.

Figure 2c shows the calculations on dependence of α_{E31}^T on temperature T as a function of magnetic field, where t_i/t, K_i, and μ_i are given as 0.06, 2.0 GPa, and 1.0 GPa, respectively, all within reasonable regions. One can find that, when considering the influence of interfacial binder layer, the calculations are in broad agreement with the experimental results. Comparison between Fig. 2b and c reveals that the interface effect on ME response is very remarkable in the present phase-transformation-assisted bilayer Ni_2MnGa/PZT composite. This indicates that the significant interface effect should be commonly existed in all the laminated ferromagnetic/ferroelectric multiferroic composites.

The significant influence of interfacial binder layer could be further revealed from Fig. 3. Figure 3a, b shows the dependence of ME coefficient on the relative thickness of the Ni_2MnGa layer, t_m/t, as a function of t_i/t and μ_i, respectively. Figure 3c, however, shows the α_{E31}^T versus

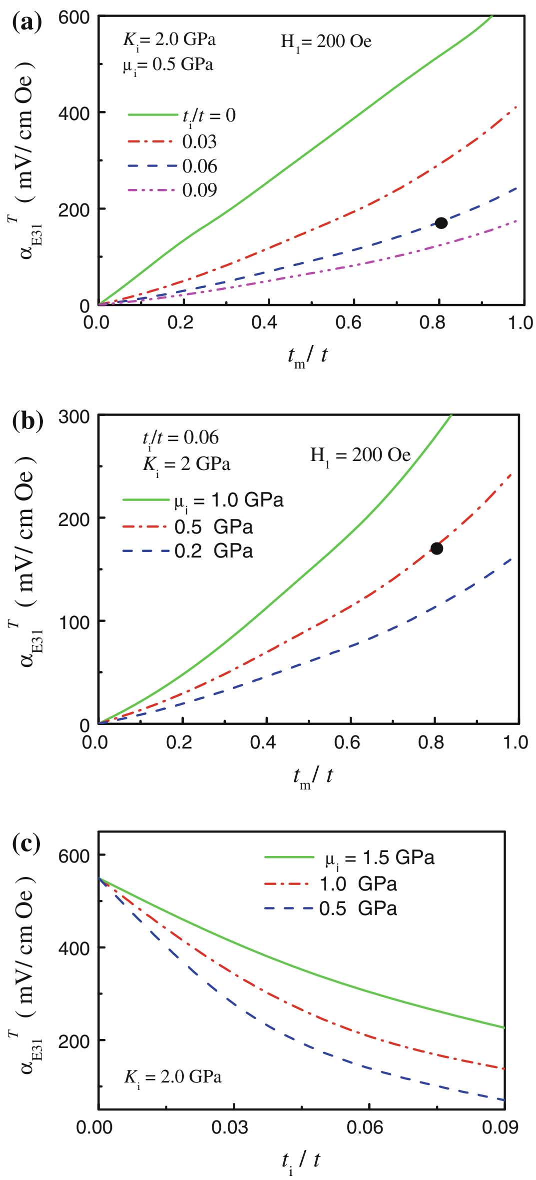

Fig. 3 Dependence of α^T_{E31} of the bilayer Ni_2MnGa/PZT composites on the relative thickness of Ni_2MnGa layer (t_m/t) as a function of the relative thickness (t_i/t) **(a)** and shear modulus (μ_i) of the interface binder layer. **c** Dependence of α^T_{E31} of the bilayer Ni_2MnGa/PZT composites on t_i/t as a function of μ_i. *Dots* are experiment results [34] and curves are from present calculations

t_i/t curves under different μ_i but constant $t_m/t = 0.8$. As seen from these figures, the ME response of the laminated composites is significantly dependent on both t_i/t and μ_i. A thick layer (i.e., larger t_i/t) of interfacial binder with low μ_i (i.e., softer binder) leads to a remarkable decrease in the ME response of the composites, especially at high t_m/t. This remarkable decrease in the ME response is mainly attributed to two reasons. The one is that the introduction of a soft binder layer results in a loss in strain transfer at Ni_2MnGa/PZT layers. The other is that the epoxy layer is inert, i.e., neither magnetostricitve nor piezoelectric.

The enhancement in ME effect with increasing the relative thickness of Ni_2MnGa layer (Fig. 3a, b) could be reasonably explained because the mechanical interaction in the laminated multiferroic composites will be improved by a thicker strain-donor Ni_2MnGa layer bonded with a thinner strain-acceptor PZT layer. A similar conclusion has been also drawn in other calculations based on both Green's function technique [37] and constitutive equations [38]. Especially, a much more clear expression could be derived from the latter calculations to describe the dependence of α_{E31} on t_m as follows [38, 39]:

$$\alpha_{31} = -\frac{\boldsymbol{E}_3}{H_1} = \frac{t_m q^m_{11}(\boldsymbol{e}^p_{33}c^p_{31} - \boldsymbol{e}^p_{31}c^p_{33})}{(1-t_m)(\Lambda^p - \boldsymbol{e}^p_{31}) - k t_m \Lambda^m} \qquad (8)$$

with $\Lambda^p = c^p_{11}\Pi + (c^p_{12} + c^p_{13})\Omega$; $\Lambda^m = c^m_{11}\Pi + (c^m_{12} + c^m_{13})\Omega$; $\Pi = \boldsymbol{e}^p_{33}\boldsymbol{e}^p_{31} + \boldsymbol{e}^p_{33}e^p_{33} - c^p_{33}\boldsymbol{\kappa}^p_{33} - c^p_{31}\boldsymbol{\kappa}^p_{33}$; $\Omega = k^p_{33}c^p_{13} - \boldsymbol{e}^p_{33}e^p_{31}$ where superscript p and m refer to the piezoelectric phase and magnetostrictive phase, respectively; q^m is the piezomagnetic coefficient of the magnetostrictive phase; k is a scaling factor ($0 < k \leq 1$) used to describe the interface effect or the loss in strain transfer when passing through the interface, i.e., $\varepsilon^p_1 = k\varepsilon^m_1$. $k = 1$ means that the strain is fully transferred from the ferromagnetic phase to the ferroelectric phase, which is defined as perfect interface. $k \to 0$ indicates that almost all strain is lost when passing through the interface. The larger is k, the better is the coupling effect between the ferromagnetic and ferroelectric phases. A larger t_m and higher k will result in a stronger ME effect, as predicted from Eq. 8, which is in good agreement with present FEM calculations.

Besides the strain transfer, the energy transformation from magnetostatic energy to electrostatic energy will be remarkably affected by the introduction of interfacial binder layer. Defining the energy transformation efficient simply as $\Phi = \frac{1}{2}\boldsymbol{\kappa}_0\boldsymbol{\kappa}^*_{ii}\boldsymbol{E}^2_i / \frac{1}{2}\mu_0\mu^*_{11}H^2_1$ (superscript asterisk refers to the effective parameter of the whole composite), the interface effect on the energy transformation efficiency in the laminated multiferroic composites is calculated as well. Figure 4 shows the dependence of Φ on t_m/t as a function of the relative thickness of interfacial binder layer, t_i/t, where all the curves have been normalized by the maximum valued at $t_m/t = 0.5$ and $t_i/t = 0$ in order to give a clear comparison. All the curves follow a saddle shape, i.e., the energy transformation efficiency varies nonmonotonically with t_m/t. Under the assumption of perfect bonding, the peak value for Φ is produced at $t_m/t = 0.5$. However, when an interfacial binder layer is introduced, the peak value will be significantly reduced. Besides, the peak value will be produced at a higher t_m/t. These results indicate that the existence of binder layer weakens the energy transformation and the thick the binder layer is, the worse the weakening on Φ is. At this point, it is strongly

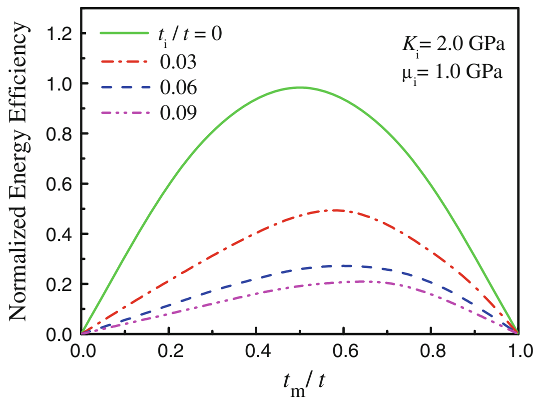

Fig. 4 Dependence of the energy transformation efficient, Φ, on t_m/t as a function of t_i/t. All the curves have been normalized by the maximum valued at $t_m/t = 0.5$ and $t_i/t = 0$ in order to give a clear comparison

suggested that interface effect should be sufficiently considered in investigating the ME effect in laminated multiferroic composites. On the other hand, the interface effect revealed in present calculations could be also employed to explain the different ME coefficient reported in previous works on the laminated multiferroic composites (e.g., [7]).

It should be addressed that the broad agreement between the calculations with the experiment results (Fig. 2c) indicates that the present method is applicable to calculate the phase-transformation-assisted ME effect in the laminated multiferroic composites.

Further prediction from present model

The NiMnGa used in Zhao et al.'s experiments [34] is polycrystalline, which have a magnetic-field-induced strain (MFIS) much smaller than single crystal NiMnGa. Subsequently, the MFIS-aided ME will be predicted by using the present model and choosing single crystal NiMnGa as the ferromagnetic phase.

It is simply assumed that the single crystal NiMnGa/PZT composite has the same geometrical configurations as presented in Fig. 1. Figure 5a is the strain–temperature curve measured with a magnetic field $H_1 = 1.2$ T applied in [100] direction of single crystal $Ni_{52}Mn_{24}Ga_{24}$ [29]. The maximum field-induced strain is up to 1.5×10^4 ppm at T ~ -5 °C, which is much higher than that achieved in polycrystal NiMnGa (referring to Fig. 2a). Calculations results on ME show that a high ME coefficient close to 1×10^3 mV/cm Oe (~ 1 V/cm Oe) can be produced in the case of perfect interface bonding, see the solid curve in Fig. 5b. When the influence of interfacial binder layer is considered, the ME will be reduced because a loss in strain transfer will occur through the interface layer. One can see from Fig. 5b that, the smaller is the shear modulus, the more is the reduction in ME coefficient compared to the perfect interface case. This trend is similar to what revealed from Fig. 3.

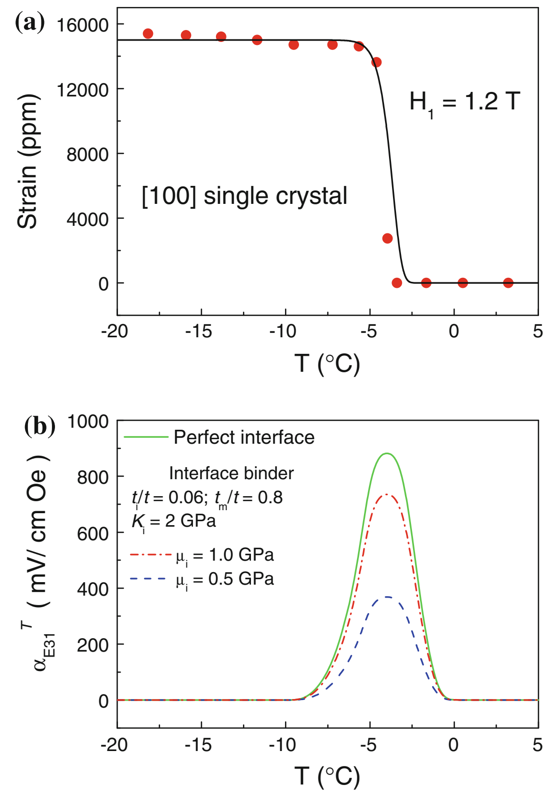

Fig. 5 **a** Dependence of the magnetic-field-aided martensite transformation on temperature for $Ni_{52}Mn_{24}Ga_{24}$ single crystal, with magnetic field $H_1 = 1.2$ T applied in [100] direction. *Dots* are experimental results [29] and *curves* are fitting ones. **b** Predicted dependence of α^T_{E31} of the single crystal $Ni_{52}Mn_{24}Ga_{24}$/PZT composite on interfacial condition (perfect interface and interfacial binder layer with high and low shear modulus) as a function of temperature

Next, another stress-induced martensite of Fe_7Pd_3 will be theoretically used as the ferromagnetic phase in the magnetoelectric composite. Cui et al. [40] measured the magnetostriction of Fe_7Pd_3 single crystal within the temperature range from 40 °C to 5 °C and found that, with the application of a compressive stress of $\sigma_1^{\text{pre}} = -1$ MPa (insert in Fig. 6a) and H_1 $\sim$2000 Oe, the striction increased with reducing temperature until to reach a value over 4×10^3 ppm at T $\sim$5 °C (Fig. 6a). Because of the existence of pre-applied stress, the constitutive equation should be further modified to include σ_1^{pre}. Equation 4 is now revised as

$$\begin{aligned} \sigma_{kl} &= c^{H,E,T}_{klij}\varepsilon_{ij} - \boldsymbol{e}^{H,T}_{ikl}\boldsymbol{E}_i - c^{H,E,T}_{klij}\varepsilon^{M}_{ij} + \sigma^{\text{pre}}_{kj}, \\ \boldsymbol{D}_k &= \boldsymbol{e}^{H,T}_{kij}\varepsilon_{ij} + \boldsymbol{\kappa}^{H,\varepsilon,T}_{ki}\boldsymbol{E}_i + \alpha^{T}_{ki}H_i, \\ B_j &= \mu_{ji}(\varepsilon, \boldsymbol{E}, H, T)H_i, \end{aligned} \tag{9}$$

The above constitutive equations have the features: (i) the non-linear striction depend not only on magnetic field

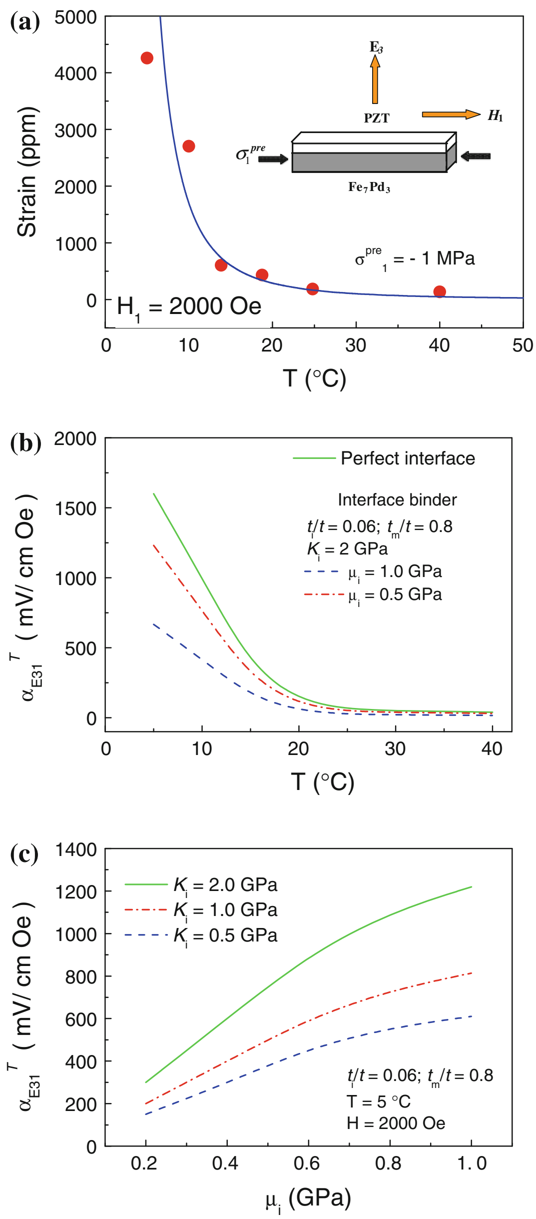

Fig. 6 **a** Dependence of the magnetic-field-aided martensite transformation on temperature for Fe_7Pd_3 single crystal under magnetic field $H_1 = 2000$ Oe. *Dots* are experimental results [40] and curves are fitting ones. Inset is to show the direction of pre-stress. **b** Predicted dependence of α_{E31}^{T} of the Fe_7Pd_3/PZT composite on interfacial condition (perfect interface and interfacial binder layer with high and low shear modulus) as a function of temperature. **c** Predicted dependence of α_{E31}^{T} of the Fe_7Pd_3/PZT composite on K_i (bulk modulus of the interfacial binder layer) as a function of μ_i (shear modulus of the interfacial binder layer) at $T = 5$ °C

but also on temperature, and (ii) incorporation of pre-existed stress. Similar modification can be made in the traditional magneto-electro-elastic coupling constitutive equations to include the influence of residual stress, and/or pre-existed electric displacement, and/or magnetic induction. Based on the $\varepsilon - T$ curve in Fig. 6a and still using PZT as the ferroelectric phase, calculations on ME are performed by employing Eq. 9. The results, without and with the consideration of interfacial binder layer, are, respectively, shown in Fig. 6b. It is interesting to find that the ME coefficient of Fe_7Pd_3/PZT composite will exceed 1×10^3 mV/cm Oe when the temperature below about 10 °C. Even with the interfacial binder layer, the ME coefficient of the composite can be close to 1×10^3 mV/cm Oe if the binder has a somewhat high shear modulus (such as $\mu_i = 1.0$ GPa in Fig. 6b).

The above predictions using present model clearly shown that a high ME coefficient up to $\sim 1 \times 10^3$ mV/cm Oe may be achieved in the phase-transformation-aided ferromagnetic/ferroelectric composites. But, as we can see from Fig. 6c, the ME coefficient is remarkably dependent on the characteristics of the interfacial binder layer. The binder with a high μ_i as well as a high K_i is required to produce a giant ME effect.

Conclusions

The ME effect of laminated magnetostrictive/piezoelectric multiferroic composites is remarkably dependent on the thickness and characteristics of binder layer. Based on revised constitutive equations, calculations have been performed on $Ni_{47.4}Mn_{32.1}Ga_{20.5}$/PZT bilayer composites to investigate the combined effect of the binder layer thickness and layer characteristics on the ME effect. Results show that, when the interface layer is somewhat stiff and the binder layer is thin, a large ME effect should be produced. Further predictions using present model reveal that the usage of single crystal Fe_7Pd_3 as ferromagnetic phase to form magnetoelectric composite with PZT can produce a high ME up to ~ 1 V/cm Oe.

Acknowledgements This work was supported by the National Basic Research Program of China (Grant No. 2010CB631003) and the National Natural Science Foundation. This work was also supported by the 111 Project of China under Grant No. B06025 and the Fundamental Research Funds for the Central Universities.

Appendix: The procedure of finite element analysis

(1) Software: Ansys 7.0;
(2) Element type: coupled-field solid element is chosen to calculate the mechanical-electric coupling;
(3) Material properties: a complete description of constitutive relationship of the ferroelectric phase includes the anisotropic elastic matrix, piezoelectric matrix, and dielectric matrix. That of the ferromagnetic phase includes the anisotropic elastic matrix, magnetostrictive curve and permeability matrix. The properties

can be referred to Table 1. Because the magnetostrictive curve is nonlinear, the curve will be discretized. The magnetic-field-induced strain will be directly loaded on the ferromagnetic phase with the application of the magnetic field. The elastic constant of polymer binder can be determined from the expressions of $K_i = (c^i_{11} + 2c^i_{12})/3$ and $\mu_i = (c^i_{11} - c^i_{12})/2$, together with the defined values for K_i and μ_i;

(4) Modeling and meshing: the geometrical configuration of the tri-layer composite is shown in Fig. 1. Only 1/4 of the symmetric composite is used in the modeling in order to short the calculation time. The bonding between the layers are performed by the glue operation in Ansys;

(5) Boundary condition and loading: all the symmetric planes in the 1/4 model have zero displacements either in X_1 or X_2 direction. The upper surface of PZT and bottom surface of NiMnGa have zero displacement in X_3 in according to the clamping constraint. The discretized magnetostriction is directly applied on the NiMnGa phase and the corresponding magnetic field is also applied.

(6) Solution: the finite element equations are solved using current LS in the Ansys;

(7) Post-process: averaging the parameters of stress, strain, electric field, etc, over the whole sample to yield the average values;

(8) Determined ME coefficient: putting the average values obtained in (7) into Eq. 4 to determined α^T_{ij}.

References

1. Fiebig M, Lottermoser Th, Frohlich D, Goltsev AV, Pisarev RV (2002) Nature 419:818
2. Kimural T, Goto T, Shintani H, Ishizaka K, Arima T, Tokura Y (2003) Nature 426:55
3. Ramesh R, Spaldin NA (2007) Nat Mater 6:21
4. Wang J, Neaton JB, Zheng H, Nagarajan V, Ogale SB, Liu B, Viehland D, Vaithyanathan V, Schlom DG, Waghmare UV, Spaldin NA, Rabe KM, Wuttig M, Ramesh R (2003) Science 299:1719
5. Spaldin NA, Fiebig M (2005) Science 309:391
6. Eerenstein W, Mathur ND, Scott JF (2006) Nature 442:759
7. Fiebig M (2005) J Phys D 38:R123
8. Freeman AJ, Schmid H (1975) Magnetoelectric interaction phenomena in crystals. Gordon and Breach, London
9. Dzyaloshinskii IE (1960) Sov Phys JETP 10:628
10. Folen VJ, Rado GT, Stalder EW (1961) Phys Rev Lett 6:607
11. Bichurin M (ed) (1997) Proceedings of the 3rd international conference on magnetoelectric interaction phenomena in crystals MEIPIC-3 (Novgorod, Russia), Ferroelectric, vol 204, p 1
12. Hill NA (2000) J Phys Chem B 104:6694
13. Van Aken BB, Palstra TTM, Filippetti A, Spaldin NA (2004) Nat Mater 3:164
14. Lottermoser T, Lonkai T, Amann U, Hohlwein D, Ihringer J, Fiebig M (2004) Nature 430:541
15. Rado G, Ferrari JM, Maisch WG (1984) Phys Rev B 29:4041
16. Harshe G, Dougherty JP, Newnham RE (1993) Int J Appl Electromagn Mater 4:161
17. Nan CW (1994) Phys Rev B 50:6082
18. Bichurin MI, Filippov DA, Petrov VM, Laletsin VM, Paddubnaya N, Srinivasan G (2003) Phys Rev B 68:132408
19. Srinivasan G, Rasmussen ET, Levin BJ, Hayes R (2002) Phys Rev B 65:134402
20. Dong SX, Li JF, Viehland D (2004) Appl Phys Lett 85:2307
21. Srinivasan G, Zavislyak IV, Tatarenko AS (2006) Appl Phys Lett 89:152508
22. Dong SX, Zhai JY, Bai FM, Li JF, Viehland D (2005) Appl Phys Lett 87:062502
23. Ryu J, Priya S, Carazo AV, Uchino K, Kim HE (2001) J Am Ceram Soc 84:2905
24. Mori K, Wuttig M (2002) Appl Phys Lett 81:100
25. Engdahl G (2000) Handbook of giant magnetostrictive materials. Academic Press, New York
26. Dong SX, Li JF, Viehland D (2003) Appl Phys Lett 83:2265
27. Dong SX, Zhai JY, Li JF, Viehland D (2006) Appl Phys Lett 89:252904
28. Zhai JY, Dong SX, Xing ZP, Li JF, Viehland D (2006) Appl Phys Lett 89:083507
29. Wang WH, Wu GH, Chen JL, Yu CH, Gao SX, Zhan WS, Wang Z, Gao ZY, Zheng YF, Zhao LC (2000) Appl Phys Lett 77:3245
30. Zuo F, Su X, Wu KH (1998) Phys Rev B 58:11127
31. Liu G, Nan CW, Cai N, Lin YH (2004) J Appl Phys 95:2660
32. Liu G, Nan CW, Cai N, Lin YH (2004) Int J Solids Struct 41:4423
33. Nan CW, Lin YH, Huang JH (2001) Phys Rev B 63:144415
34. Zhao K, Chen K, Dai YR, Wan JG, Zhu JS (2005) Appl Phys Lett 87:162901
35. Planes A, Obradó E, Gonzàlez-Comas A, Mañosa Ll (1997) Phys Rev Lett 79:3926
36. Stipcich M, Mañosa Ll, Planes A, Morin M, Zarestky J, Lograsso T, Stassis C (2004) Phys Rev B 70:054115
37. Nan CW, Liu G, Lin YH, Chen HD (2005) Phys Rev Lett 94:197203
38. Liu G, Nan CW, Sun J (2006) Acta Mater 54:917
39. Harshe G (1991) Ph. D Thesis, The Pennsylvania University
40. Cui J, Shield TW, Wuttig M (2004) Appl Phys Lett 85:1642